CONF-800531--8

LA-UR 80-1327

TITLE: CALCULATION OF ^{59}Co NEUTRON CROSS SECTIONS BETWEEN 3 and 50 MeV

AUTHOR(S): E. D. Arthur, P. G. Young, and W. E. Matthes

SUBMITTED TO: Symposium on Neutron Cross Sections from 10 to 50 MeV

Brookhaven National Laboratory
May 12-14, 1980

los alamos
scientific laboratory
of the University of California
LOS ALAMOS, NEW MEXICO 87545

Form No. 836
R4 Jan. 79
UCD

UNITED STATES
ENERGY RESEARCH AND
DEVELOPMENT ADMINISTRATION
CONTRACT W-7405-ENG-36

CALCULATION OF ^{59}Co NEUTRON CROSS SECTIONS BETWEEN 3 and 50 MeV*

E. D. Arthur and P. G. Young

Theoretical Division
Los Alamos Scientific Laboratory
University of California
Los Alamos, New Mexico 87545

and

W. K. Matthes

EURATOM CCR
Ispra, Italy

ABSTRACT

Knowledge of the ^{59}Co (n,p), (n,α), and (n,xn) cross sections up to 50 MeV are necessary to satisfy priority dosimetry data needs of the FMIT facility. Since experimental data extend only to 25 MeV in the case of (n,xn) reactions (and lower for the others), we calculated these cross sections as well as those from competing reactions for neutron energies between 3 and 50 MeV. Neutron optical parameters were determined that were valid from several hundreds of keV to 50 MeV. Other parameters were determined or verified through analysis of various experimental data types, thus providing the basis for complete and consistent nuclear model calculations of n + ^{59}Co reactions.

INTRODUCTION

To characterize the neutron environment of samples irradiated in the neutron flux of the Fusion Materials Irradiation Test Facility, dosimetry reaction cross sections must be known to neutron energies of 50 MeV. Since the ^{59}Co (n,p), (n,α), and (n,xn) cross sections represent priority candidates for dosimetry reactions spanning the energy range of interest to materials damage studies, we

*Work supported by the U.S. Department of Energy and EURATOM.

performed calculations of neutron reactions on ^{59}Co between 3 and 50 MeV. In contrast to our earlier work [1] in which cross sections were calculated to 40 MeV using global optical parameter sets, we have devoted a large effort to the determination and verification of parameters suitable for calculations over this energy range. The constraints placed by the data used in this process should result in an improvement in the reliability of the calculated cross sections.

PARAMETER DETERMINATIONS

Our efforts to determine or verify neutron or charged-particle optical parameters generally follow the steps employed in our recent ^{54,56}Fe calculations. [2] That is, quite a large effort has been made through fitting techniques to find neutron optical parameters valid over the entire energy range between several hundred keV and 50 MeV (in this instance). For proton and alpha emission we have generally modified existing parameter sets and then verified their applicability through comparison to independent data types.

To determine our neutron optical parameters, we used ^{59}Co total cross-section data between 0.5 and 30 MeV, supplemented at higher energies by estimates based on iron total cross section to 50 MeV. Constraints on the low energy behavior of the parameters were achieved through use of s- and p-wave strength functions as well as values for the potential scattering radius. Elastic-scattering angular distribution data were included for neutron energies of 8, 11, and 15 MeV, along with 14-MeV reaction cross sections. Around 40 MeV, an estimate for the reaction cross section was included based on recent data [3] from n + Fe reaction cross-section measurements. For the fit, two energy regions were used with the boundary chosen at 6 MeV. The resulting parameters are shown in Table 1. To fit the data, a surface derivative Woods-Saxon potential was used having a positive energy coefficient at low energies with a negative coefficient for energies above 6 MeV. A volume imaginary potential was also used that became dominant for neutron energies above 25 MeV. The calculated total and elastic cross sections are compared to experimental data in Figs. 1-a and 1-b, respectively.

For protons and alphas we used modifed forms, respectively, of the Percy [4] and Lemos [5] global parameter sets that were derived during our n + ^{54,56}Fe calculations (see contribution to these proceedings). To further verify them for this problem, we made Hauser-Feshbach calculations of ^{57}Fe (p,n) and ^{55}Mn (α,n) cross sections (with the neutron parameters of Table I) that are compared to data [6-8] in Figs. 2 and 3.

Other quantities required for these calculations consisted mainly of gamma-ray transmission coefficients, level density parameters, and parameters needed for preequilibrium corrections. The latter two parameter types were taken from published values since these result generally from the examination of systematic behavior of pertinent data. We employed the Gilbert-Cameron [9] level density expressions along with the Cook [10] values for Fermi-gas parameters and adjusted constant temperature parameter values to fit (for each nucleus in the calculation) information pertaining to the cumulative number of levels occurring up to a given excitation energy. Since constant-temperature level-density expressions were often employed up to fairly high excitation energies, uncertainties in the level-density expressions, occurring mainly in the Fermi-gas portions, could be minimized.

The matrix normalization constant needed to fix transition rates in the master equations preequilibrium model was taken from the value recommended by Kalbach [11]. The form of the absolute square of this residual two-body matrix element was assumed to be dependent on both the excitation energy available per exciton and the compound system mass [12].

Gamma-ray transmission coefficients were calculated assuming a giant dipole resonance form and were normalized through determination of the gamma-ray strength function by fits to ^{59}Co (n,γ) data. This method eliminates much of the uncertainty occurring from normalization to $2\pi\langle\Gamma_\gamma\rangle/\langle D\rangle$ ratios, especially for nuclei where no such data are available. The ^{60}Co gamma-ray strength function was very similar in magnitude to values we determined for ^{55}Fe and ^{57}Fe. [2]

CALCULATIONS AND RESULTS

The above parameters, along with discrete-level information, were used with three nuclear models--Hauser-Feshbach, preequilibrium, and direct-reaction--that describe the main features of most neutron reactions occurring in this mass and energy region. The main nuclear model codes used for the calculations were CONNUC, [13] GNASH, [14] and DWUCK. [15] In addition to Hauser-Feshbach calculations to which width fluctuations (CONNUC) and preequilibrium corrections (GNASH) were applied, a small direct-reaction component was determined for the first several inelastic levels through DWBA calculations (DWUCK). A weak coupling model for ^{59}Co consisting of a spin 7/2 hole outside a ^{60}Ni core was used along with the assumption of $\ell = 2$ transfer and a value of $\beta_2 = 0.2$. That this model was adequate to represent ^{59}Co direct cross sections was verified by examination of the relative magnitude and shape of 11 MeV proton inelastic scattering data [16] to several low-lying levels.

Figure 4 presents a general overview of the calculated cross sections. Since alpha decay chains were not followed individually except off the main neutron branch, contributions to (n,nα), (n,2nα), etc. cross sections were not ascertained for all components at higher incident energies. However, the effect of this approximation on total alpha production is very small. Also, reactions involving multiple proton emission such as (n,xnyp) ($y \geq 2$) were not included since tests performed at 40 MeV indicated that proton emission comprised less than a few percent of the total cross section for decay of a given compound nucleus occurring along the proton branch included in the calculations.

With reference to these cross sections, several general features are noteworthy. At higher energies, reactions involving proton emission such as (n,3np) dominate because of the multiple reaction paths that can produce the final nucleus. Also the compound systems produced along the main neutron decay chain tend to be more proton rich, resulting in less neutron emission. Thus, the (n,4n) reaction that has been suggested for dosimetry uses at higher neutron energies may suffer from a low cross-section value. Reactions such as (n,p), (n,2n), and (n,3n) maintain their cross-section magnitudes without rapid decreases after competing channels become available at higher energies. This results from preequilibrium effects and is well documented from the behavior of (p,xn) and (p,pxn) cross sections in this energy region.

Calculated values for ^{59}Co neutron reactions of dosimetry interest are compared to data in the next several figures. Figure 5 illustrates calculated (n,xn) cross sections with available data [17-21] [(n,2n) and (n,3n) measurements shown here were made using scintillator tanks]. Similarly, in Fig. 6 comparisons are made to ^{59}Co (n,2n) data measured by activation techniques. Both the (n,2n) and (n,3n) threshold energy regions provide an opportunity to verify the low-energy neutron transmission coefficients since emission to discrete states in the residual nucleus dominates here.

The slope of the calculated cross sections, particularly around the (n,2n) threshold, depends strongly upon competition from gamma-ray and charged-particle emission. The fact that the calculations fit the steeply rising cross section around the (n,2n) threshold provides verification of the normalization used for gamma-ray transmission coefficients since the (n,n'γ) reaction competes most strongly there. In the (n,3n) threshold region, such effects are reduced because of increased competition from particle emission through the (n,np) or (n,2n) reactions.

Figure 7 illustrates calculated and experimental values for the ^{59}Co (n,p) reaction. At lower energies, the behavior of the proton transmission coefficients calculated using the modified Perey optical parameters plays an important role in the agreement obtained with the data of Smith [22] (closed circles). At 14 MeV

the calculations fall somewhat lower than the experimental data, most of which cluster around cross-section values of approximately 50–60 mb. Attempts to increase the calculated values in this energy region through adjustment of level density parameters for ^{59}Fe began to disturb the agreement achieved at lower energies. In making such adjustments, the (n,pn) cross section was also increased, adding to the competition to the (n,p) reaction. These two factors made it difficult to adjust these parameters to achieve an increase in the calculated (n,p) values. Potential problems may exist in the relative amounts of proton and neutron emission predicted by the preequilibrium model. However, comparisons of our calculations to available proton emission spectra and (n,p) cross sections for nearby nuclei have resulted in good agreement, particularly between 15 and 20 MeV.

Although (n,np) + (n,pn) reactions are not of interest with respect to dosimetry cross sections, competition from them indirectly affects the calculated (n,2n) and (n,p) cross sections. Figure 8 illustrates our calculated (n,np) and (n,pn) cross section (solid line) and the portion of the reaction leading to the 0.811-MeV gamma ray in ^{58}Fe (dashed line). Also shown are the data of Corcalciuc et al [23] for the production of this gamma ray. The shoulder around 11–13 MeV results from the (n,np) reaction since in the ^{59}Co compound system the proton binding energy is about 3 MeV less than that of the neutron. In this region, the sub-Coulomb barrier behavior of the proton transmission coefficients is important, which led us to compare to low energy ^{57}Fe (p,n) cross sections as shown earlier in Fig. 2. Above 13–14 MeV, the (n,pn) reaction becomes the main contributor to this cross section. Our values (dashed line) agree well with the Corcalciuc data at higher energies but over-estimates it at 16 and 18 MeV. Some problems may exist in these measurements since their results for other reactions [^{56}Fe (n,2nγ) and ^{59}Co (n,2nγ)] appear to be systematically low when compared at these energies to other available data.

Figure 9 illustrates calculated and measured (n,α) cross sections available between 6 and 21 MeV. Although improvements may result from optical parameter adjustments at lower energies, the agreement is reasonable over this wide energy range. In addition to compound and pre-compound processes, we also included pickup and knockout contributions based on empirical expressions developed by Kalbach. [11] The agreement obtained at higher energies provides some verification of these parameterizations.

CONCLUSIONS

Independent data types have been used to determine or verify input parameters for use in comprehensive nuclear-model calculations of neutron reactions on ^{59}Co between 3 and 50 MeV. Results obtained in this manner generally produced good agreement when com-

pared to experimental data, particularly for (n,2n) and (n,3n) reactions up to 22 MeV. Calculated (n,2n) and (n,3n) cross sections should retain significant values at higher energies principally because of preequilibrium effects while the (n,4n) cross section is predicted to be significantly smaller because of competition from reactions involving proton emission. Uncertainty exists for the behavior of the (n,p) cross section above neutron energies of 10-11 MeV since some data are underpredicted by the calculations at 14 MeV. More experimental data (excitation functions) in the energy range from 10 to 20 MeV would be valuable towards solution of this problem. At higher energies, the (n,p) cross section is dominated by preequilibrium effects so that its magnitude remains relatively constant. Finally, the calculated (n,α) values agree reasonably with data up to 21 MeV indicating the reliability of the non-statistical reaction mechanisms used at higher energies.

REFERENCES

1. E. D. Arthur and P. G. Young, in Symposium on Neutron Cross Sections from 10 to 40 MeV, BNL-NCS-50681, Brookhaven National Laboratory, p. 467 (1977).

2. E. D. Arthur and P. G. Young, in Proc. Int. Conf. on Nuclear Cross Sections for Technology, Knoxville, TN (1979).

3. F. P. Brady and J. L. Romero, "Medium Energy Neutron Scattering and Reactions," UCD-CNL-192, UC, Davis report, p. 154 (1979).

4. F. G. Perey, Phys. Rev. 131, 745 (1962).

5. O. F. Lemos, "Diffusion Elastique de Particules Alpha de 21 a 29.5 MeV sur des Noyaux de la Region Ti-Zn," Orsay report, Series A, 136 (1972).

6. C. H. Johnson, A. Galonsky, and C. N. Inskeep, Physics Division Progress Report, ORNL-2910, Oak Ridge National Laboratory, p. 25 (1960).

7. T. Tanaka and M. Furukawa, J. Phys. Soc. Japan 14, 1269 (1959).

8. S. Tanaka et al., J. Phys. Soc. Japan 15, 545 (1960).

9. A. Gilbert and A. G. W. Cameron, Can. J. Phys. 43, 1446 (1965).

10. J. L. Cook, H. Ferguson, and A. R. de L. Musgrove, Aust. J. Phys. 20, 447 (1967).

11. C. Kalbach, Z. Phys. A283, 401 (1977).

12. C. Kalbach, Z. Phys. A287, 319 (1978).

13. C. L. Dunford, "A Unified Model for Analysis of Compound Nucleus Reactions," AI-AEC-12931, Atomics International report (1970).

14. P. G. Young and E. D. Arthur, "GNASH: A Preequilibrium Statistical Model Code for Calculation of Cross Sections and Emission Spectra," LA-6947, Los Alamos Scientific Laboratory report (1977).

15. P. D. Kunz, "DWUCK: A Distorted Wave Born Approximation Program," unpublished.

16. J. K. Dickens, F. G. Perey, and R. J. Silva, "Tabulated Differential Cross Sections for Elastic and Inelastic Scattering of 11 MeV Protons," ORNL-4182, Oak Ridge National Laboratory report (1967).

17. D. Hermsdorf et al., Kernenergie 17, 259 (1974).

18. N. Azziz and J. W. Connelley, Westinghouse report WCAP-7280 (1970).

19. P. Grabmayr and P. Hillie in Proc. Int. Conf. on Neutron Physics and Nuclear Data, Harwell, p. 204 (1978).

20. J. Frehaut and G. Mosinski in Nuclear Cross Sections and Technology, NBS Special Publication NBS 425, p. 855 (1975).

21. L. R. Veeser, E. D. Arthur, and P. G. Young, Phys. Rev. C16, 1791 (1977).

22. D. L. Smith and J. W. Meadows, Nucl. Sci. Eng. 60, 187 (1976).

23. V. Corcalciuc et al., Nucl. Phys. A307, 445 (1978).

TABLE I

n + ^{59}Co Optical Model Parameters

	r(fm)	a(fm)
$V(MeV) = 47.604 - 0.3636E - 0.0003E^2$	1.2865	0.561
$W_{vol}(MeV) = -0.072 + 0.1475E$	1.3448	0.473
$V_{SO}(MeV) = 6.2$	1.12	0.47
$W_{SD}(MeV) = 8.047 + 0.0805E$	1.3448	0.473
Above 6 MeV		
$W_{SD}(MeV) = 8.53 - 0.2509(E-6)$		

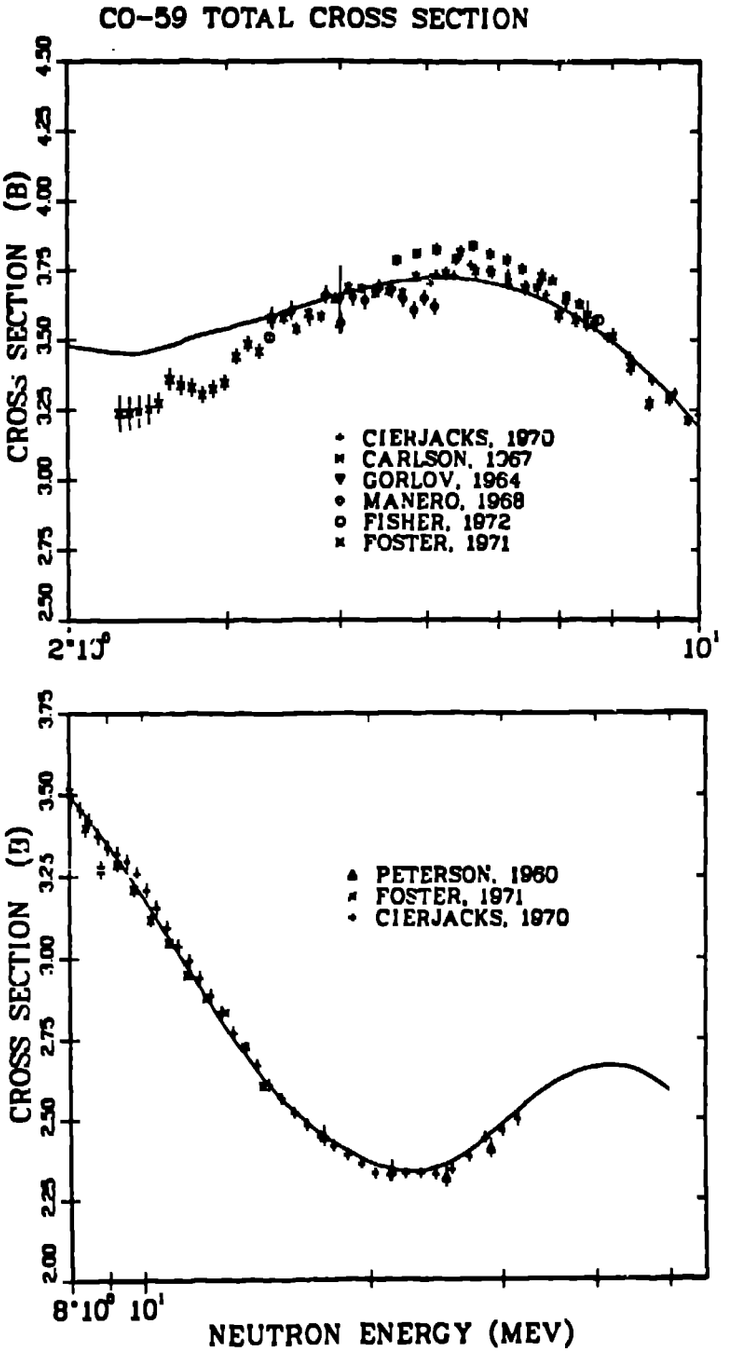

Fig. 1-a. Calculated and experimental values for the n + ^{59}Co total cross section.

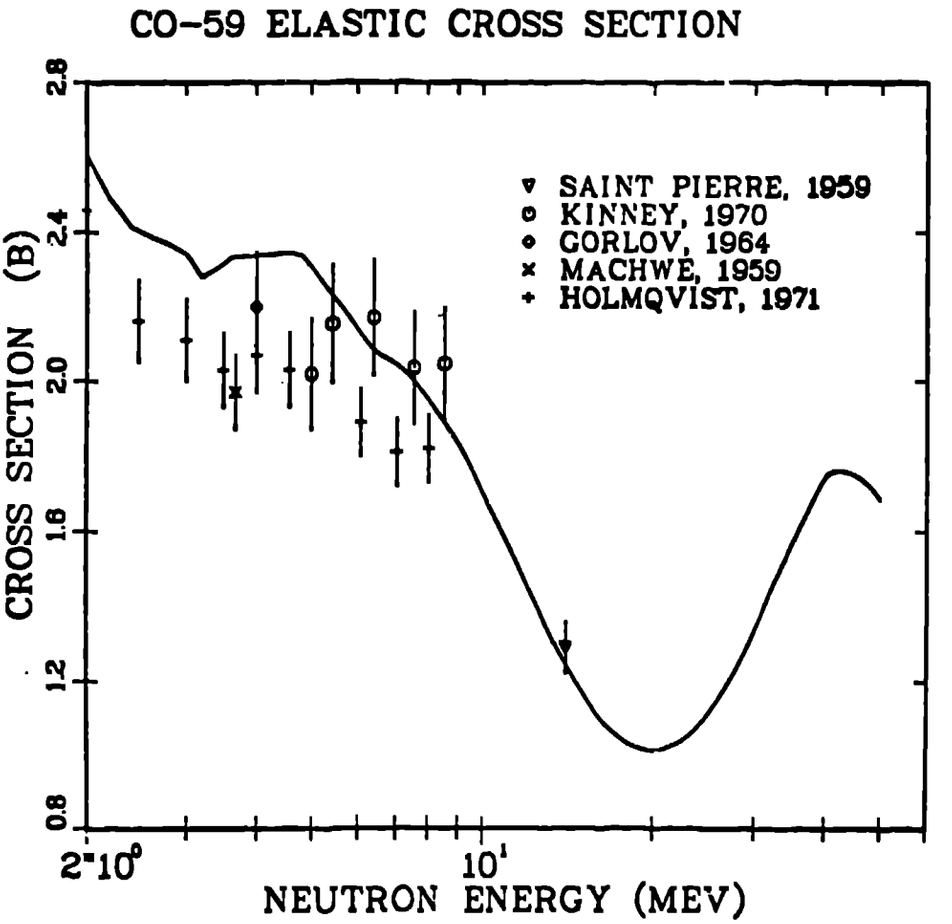

Fig. 1-b. Calculated and experimental cross sections for neutron elastic scattering from ^{59}Co.

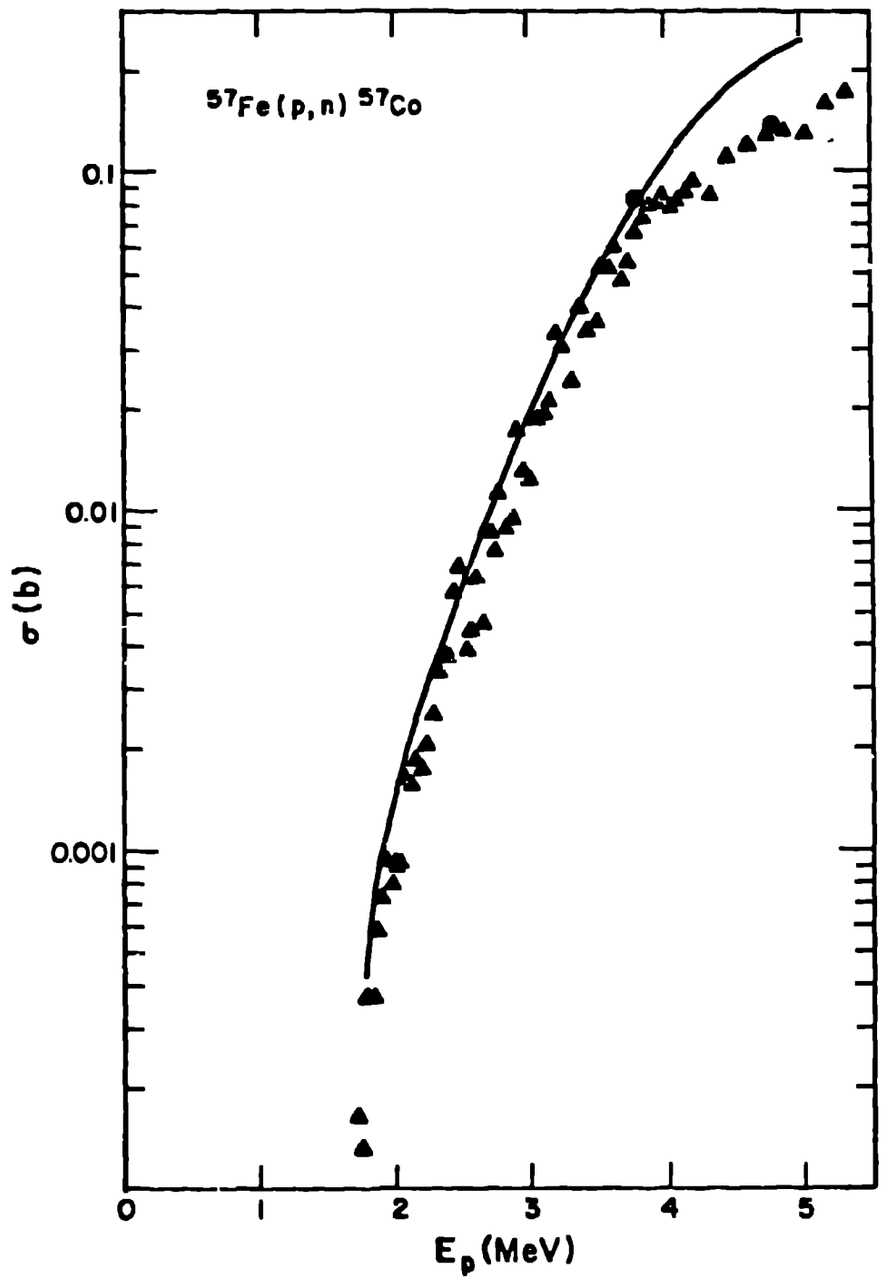

Fig. 2. Calculated and experimental $^{57}Fe(p,n)$ cross-section values. (Crosses are Ref. 6, circles are Ref. 7.)

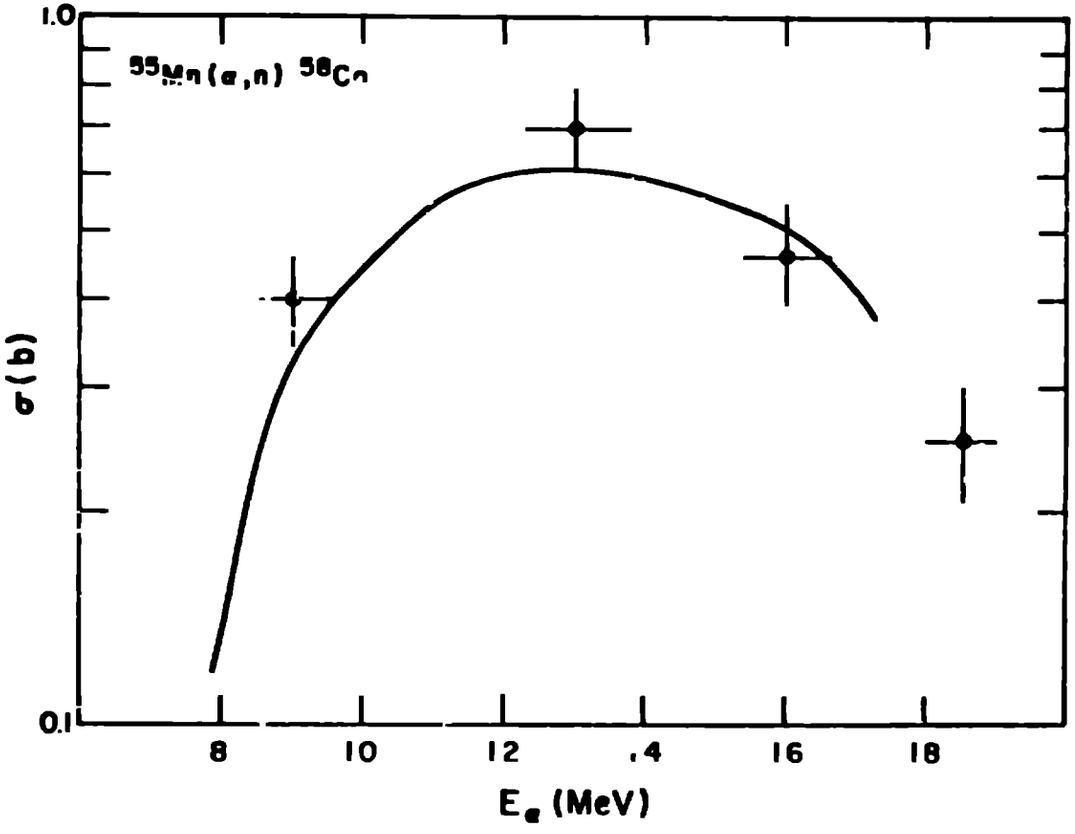

Fig. 3. The Lemos alpha-optical parameters are tested by comparison of calculated ^{55}Mn (α,n) values to experimental data (Ref. 8).

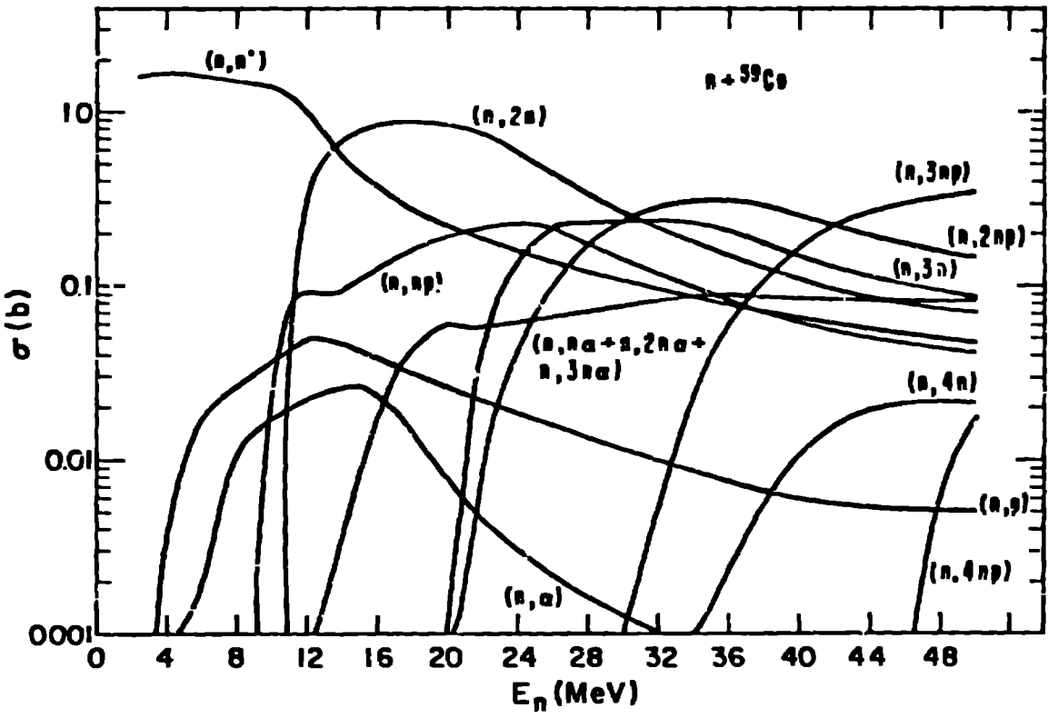

Fig. 4. Trends in cross sections calculated for ^{59}Co.

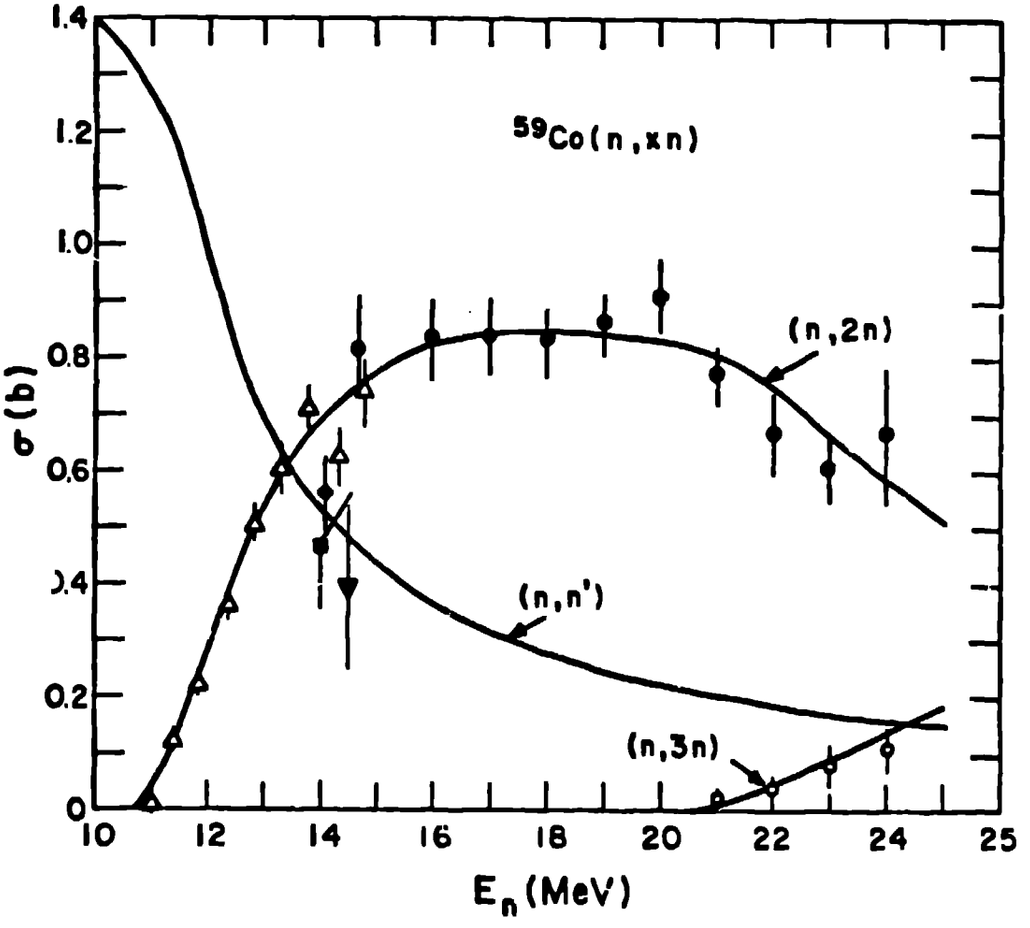

Fig. 5. Calculated and experimental (n,xn) values. For (n n') reactions, the solid diamond, aquare, and triangle represent data from Refs. 17-19. The open triangles are (n,2n) data of Frehaut (Ref. 20) while the closed and open circles are (n,2n) and (n,3n) data of Veeser (Ref. 21).

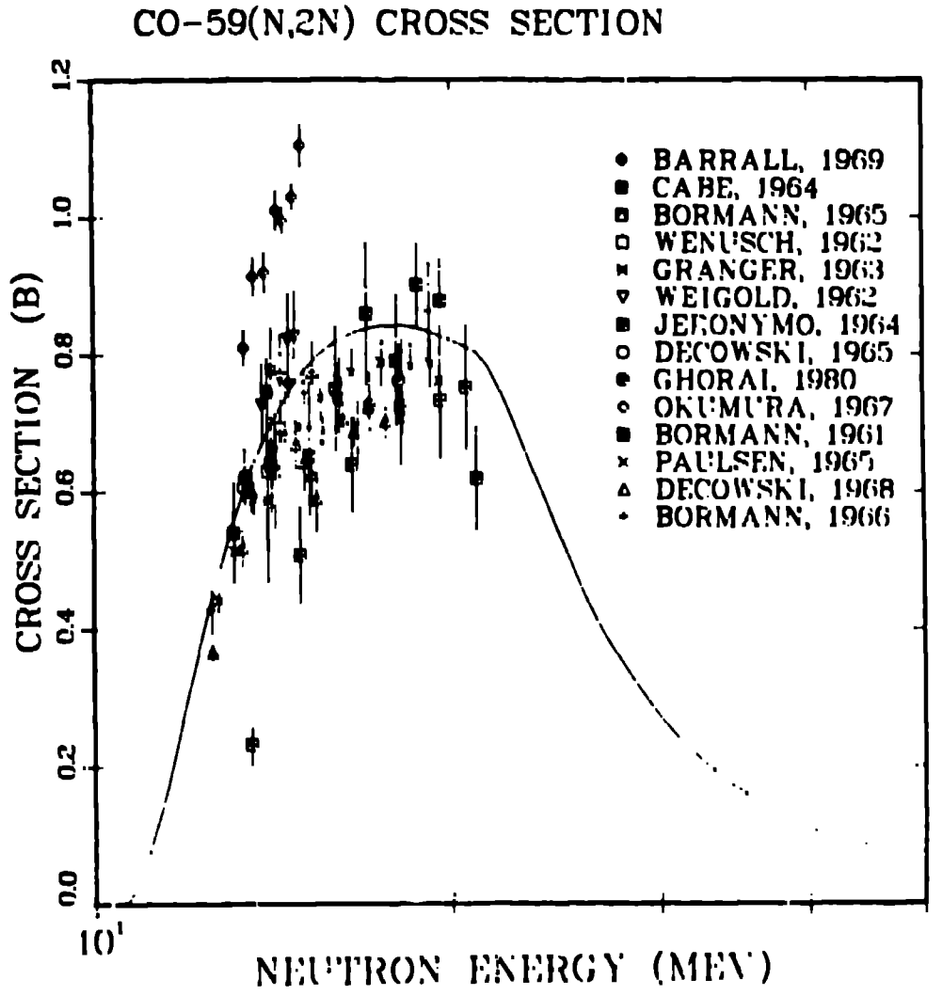

Fig. 6. Results from activation measurements of the ^{59}Co (n,2n) cross section are compared to the theoretical curve.

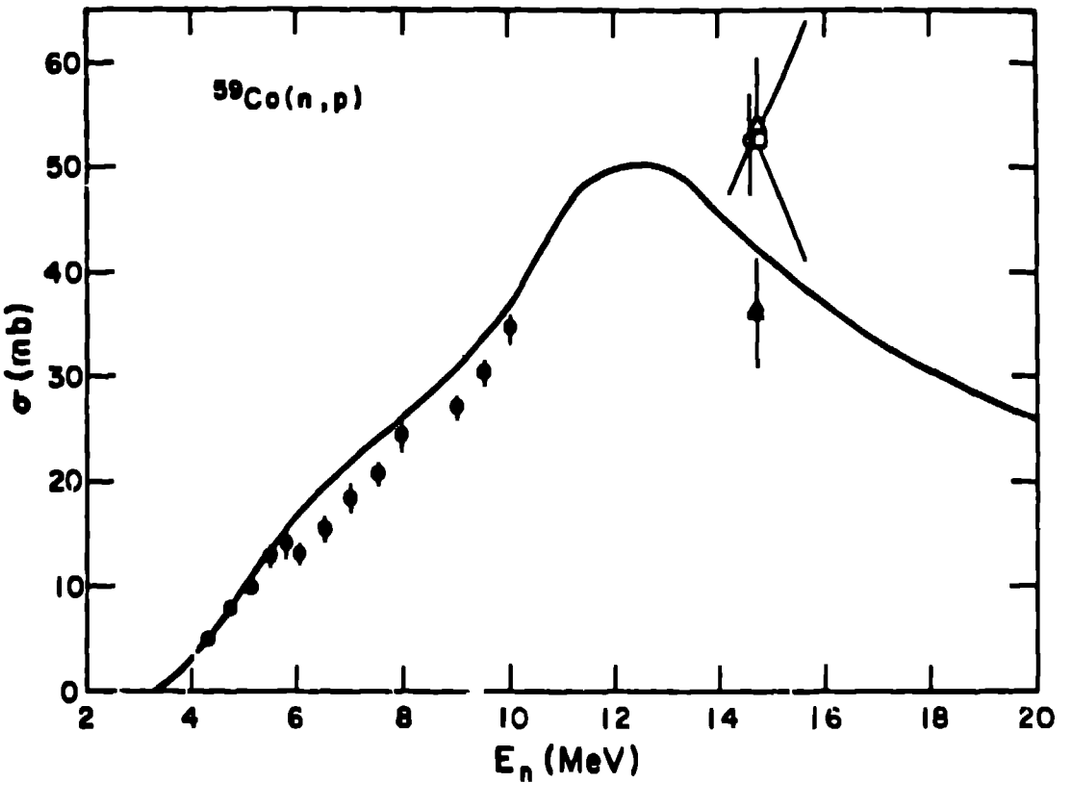

Fig. 7. Calculated and experimental values for the ^{59}Co (n,p) reaction.

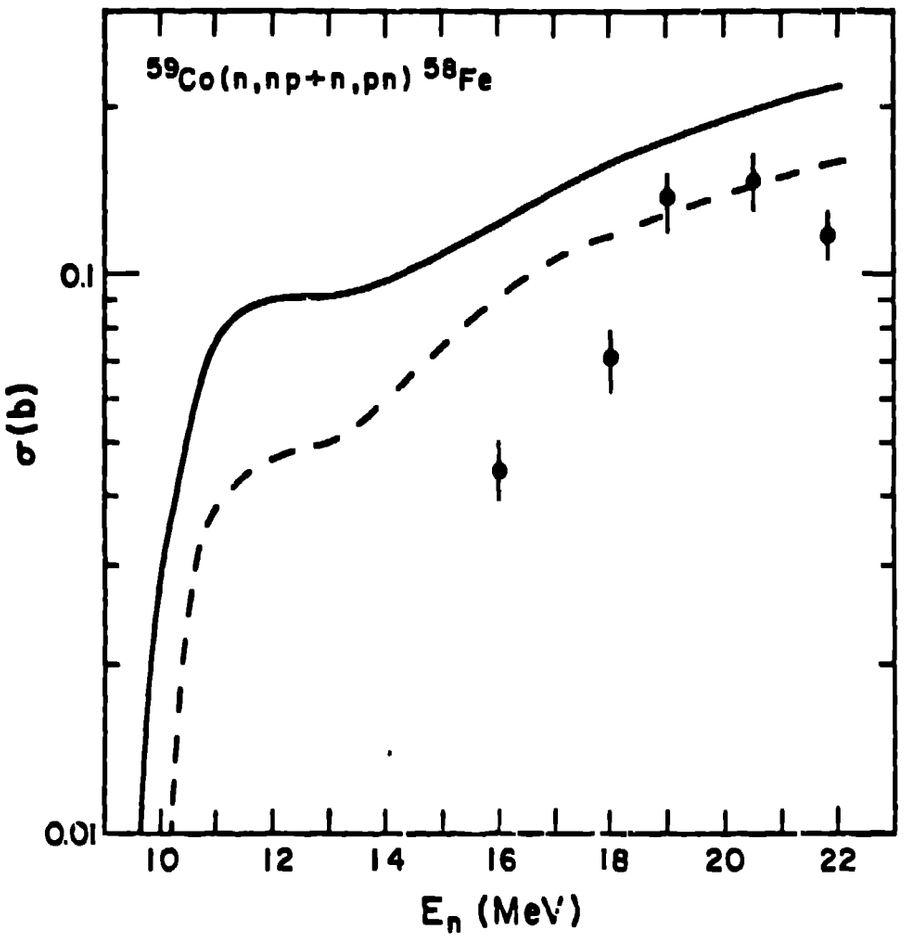

Fig. 8. The total ^{59}Co (n,np) + (n,pn) cross section (solid line) and that leading to the 0.81-MeV ^{58}Fe gamma ray (dashed line) are compared to measurements (Ref. 23) of the production cross section for that gamma ray.

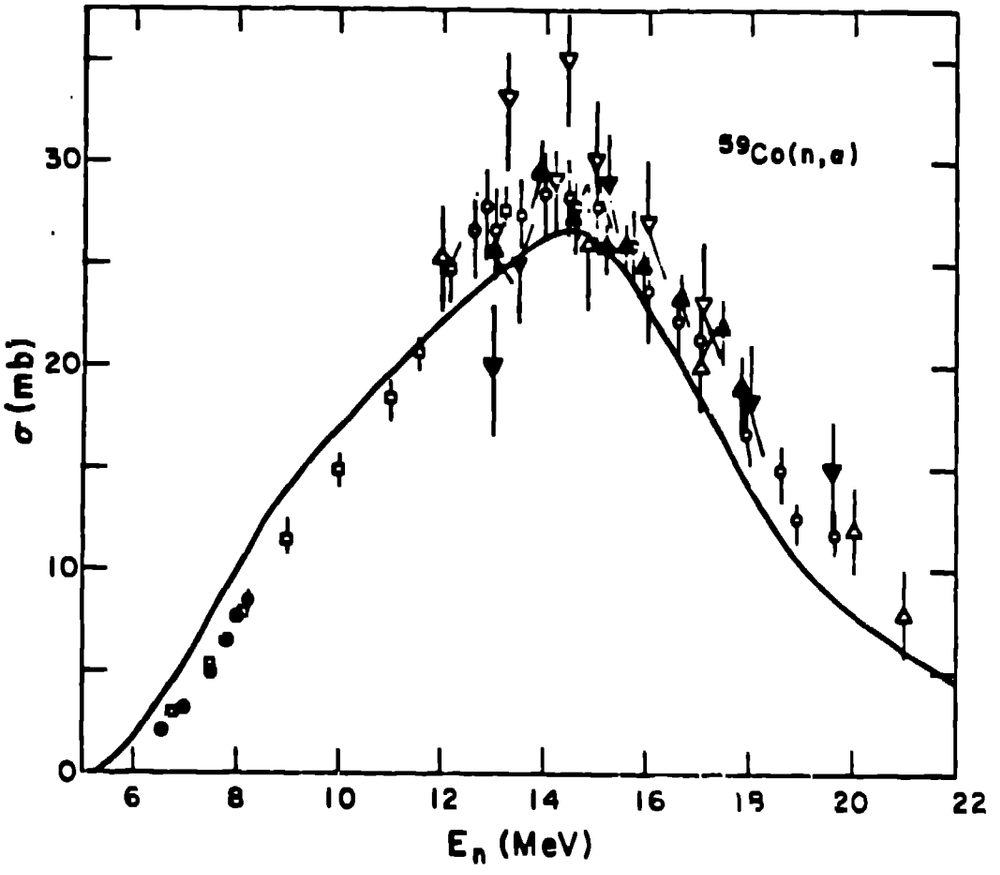

Fig. 9. Calculated and experimental ^{59}Co (n,α) values.